

Article

On the Performance of Partial LIS for 6G Systems

Mário Marques da Silva ^{1,2,3,4,*} , Ali Gashtasbi ⁵, Rui Dinis ^{2,3,5} , Gelson Pembele ^{1,2,5}, Américo Correia ^{3,6} 
and João Guerreiro ^{2,3,5} 

- ¹ Department of Engineering and Computer Sciences, Universidade Autónoma de Lisboa, 1169-023 Lisboa, Portugal; gpembele@autonoma.pt
² Autonoma TechLab, 1169-023 Lisboa, Portugal; rdinis@fct.unl.pt (R.D.); jfguerreiro@autonoma.pt (J.G.)
³ Instituto de Telecomunicações, 1049-001 Lisboa, Portugal; americo.correia@iscte-iul.pt
⁴ Ci2—Centro de Investigação em Cidades Inteligentes, 2300-313 Tomar, Portugal
⁵ Faculty of Sciences and Technology, Universidade Nova, 2829-516 Caparica, Portugal; a.gashtasbi@campus.fct.unl.pt
⁶ Department of Information Science and Technology, ISCTE-Instituto Universitário de Lisboa, 1649-026 Lisbon, Portugal
* Correspondence: mmsilva@autonoma.pt

Abstract: One of the key technologies of 6G communications relies on large intelligent surfaces (LIS), which can be viewed as a near-field beamformer that is supportive of extremely high symbol rates and enables a high level of interference avoidance. This article focuses on LIS systems, analysing the impact of the use of a whole LIS system or a subset of an antenna array. We analyse an LIS system associated with a single carrier with frequency domain equalization (SC-FDE), and with different receiver types of varying complexities. Because it is a function of the number of antennas, the computational complexity decreases when antenna elements that are closer to the user equipment are used instead of the whole LIS. Moreover, with a partial LIS, a reduction of energy consumption is achieved, and mitigation of the interference levels is obtained, allowing a performance very close to that obtained with the whole LIS system.

Keywords: LIS systems; 6G; SC-FDE; receiver types



Citation: Marques da Silva, M.; Gashtasbi, A.; Dinis, R.; Pembele, G.; Correia, A.; Guerreiro, J. On the Performance of Partial LIS for 6G Systems. *Electronics* **2024**, *13*, 1035. <https://doi.org/10.3390/electronics13061035>

Academic Editors: Oh-Soon Shin, Seung-Hoon Hwang and Junsu Kim

Received: 5 February 2024

Revised: 4 March 2024

Accepted: 7 March 2024

Published: 10 March 2024



Copyright: © 2024 by the authors. Licensee MDPI, Basel, Switzerland. This article is an open access article distributed under the terms and conditions of the Creative Commons Attribution (CC BY) license (<https://creativecommons.org/licenses/by/4.0/>).

1. Introduction

With a view to better optimizing existing resources but being associated with an even higher level of human skills, the fourth industrial revolution (also regarded as Industry 4.0) corresponds with the use of robots that replace humans and is associated with four essential terms: robotics, artificial intelligence (AI), the internet of things (IoT) and big data. The combination of these four elements is transforming the way that companies produce and provide products and services, the way society is organized, and the way human beings live [1]. It thus corresponds with the replacement of humans by machines, or their interaction [2]. Like previous industrial revolutions, it corresponds with a better optimization of existing resources. An example of this is automation, and with it the autonomous vehicle, while the massification of car sharing will be facilitated by the abolition of drivers.

The fifth generation of mobile communications (5G), given the contribution of IoT, is an important pillar of the fourth industrial revolution. With this generation, machines communicate with each other, instead of people. This is disruptive, as previous generations of communications have been limited to interconnecting humans rather than machines [3].

This fifth generation of mobile communications corresponds with the initial contribution of IoT to the fourth industrial revolution, while the sixth generation of mobile communications (6G) will correspond with an improvement in this contribution in a more significant and broad way, supporting new services such as the following:

- Holographic services;
- Extended and augmented reality;

- Location and remote-control applications and mapping;
- Future eHealth services—healthcare;
- Next-generation autonomous vehicles;
- More efficient IoT connectivity of low-power devices for smart cities and smart homes;
- Interaction with high-speed unmanned aircraft vehicles.

Meanwhile, 6G is expected to include the following requirements:

- Speeds as high as 1 terabit per second;
- Higher network capacity, supporting a much higher number of mobile devices per square kilometre;
- Lower latency, as required for delay-sensitive applications, such as autonomous driving, online gaming or controlling remote devices.

With the aim of interconnecting billions of IoT devices with extremely high throughputs and low latencies, 6G requirements are expected to be achieved using mechanisms such as block transmission techniques, advanced error correction codes and large intelligence surfaces (LIS). The LIS system can be viewed as a beyond-massive multiple input multiple output (MIMO) service, with an even higher number of antenna elements and supporting higher capacities and data rates.

Wireless communications are commonly established beyond the Fraunhofer distance, that is, in the far-field [4]. Individual antenna elements of the LIS act in the far-field, but the LIS system, as a whole, works in the near field [4–6]. Therefore, this can be viewed as a near-field beamformer, differing from a traditional beamformer because the beam can also be directed over a distance, in addition to being directed along bearing and elevation planes. This additional property allows for a reduction of interference between users that are aligned in terms of bearing and elevation but located at different distances. Note that the adjacent antenna elements of the LIS are typically spaced apart $\lambda/2$, while the channel correlation between the antenna elements allows for the creation of the above-described beam.

It is worth noting that previous works have addressed the deployment of improved capabilities (better spectral efficiency, increased data rates, lower latencies, better performances) using energy-efficient techniques, such as non-orthogonal multiple access (NOMA), that take into account the received powers. The work published in [7] investigates NOMA-assisted secure offloading for vehicular edge computing networks in the presence of multiple malicious eavesdropper vehicles. Instead of using an LIS between the user and a BS, the work published in [8] considers a full-duplex unmanned aerial vehicle relay employed to increase the communication capacity of millimetre-wave networks.

Channel encoding is proposed as a solution for handling complexity. In low-density parity-check (LDPC) codes, complexity reduction is emphasized for efficient operation in LIS scenarios. LDPC codes empower a coded MIMO system to achieve a data rate nearly approaching that of the Shannon limit. LDPC codes boast remarkable error-correction prowess while maintaining minimal decoding complexity, making them highly compatible with LIS environments.

In this article, we analyse an LIS [9–13] system associated with a single carrier with frequency domain equalization (SC-FDE) [14,15], which is an alternative to orthogonal frequency division multiplexing (OFDM). Due to the high peak-to-average power ratio (PAPR) of OFDM signals, their use in uplink scenarios is not well suited. SC-FDE transmission presents a less significant PAPR, and is thus more suited for the uplink scenario. Four different receivers are studied in this article and are compared in terms of performance: zero forcing (ZF), minimum mean squared error (MMSE), maximum ratio combining (MRC), and equal gain combining (EGC) [16,17]. Moreover, the LIS system, combined with SC-FDE transmission, is also studied in scenarios associated with LDPC codes.

This article is an extension of the research published in [10], using a subset of the antenna LIS elements (referred to as a partial LIS), instead of the whole LIS. Because it is a function of the number of antennas, the computational complexity decreases when using only antenna elements that are closer to the user equipment (UE) instead of the whole LIS. Moreover, with a partial LIS, a reduction of energy consumption is achieved, and mitigation

of the interference levels is obtained, allowing a performance that is approximately the same as that obtained with the whole LIS system.

The outline of this article is as follows: system and signal characterizations are presented in Section 2; the performance outcomes are shown and discussed in Section 3; and, finally, the conclusions of this article are presented in Section 4.

2. System and Signal Characterization

Sixth generation communications are expected to reach the requirements of a peak data rate of, at least 1 Tbps in nomadic access (100 times higher than 5G) and 1 Gbps in a mobile environment (10 times higher than 5G), while the energy efficiency is expected to be 10 to 100 times better than 5G, with a spectral efficiency 5 to 10 times better than 5G. These requirements are expected to be achieved with LIS systems associated with terahertz bands and block transmission techniques. Note that the higher the carrier frequency is, the greater the channel coherence bandwidth.

The LIS fits well with terahertz bands because the lower wavelength originates from extremely low antenna sizes, which facilitates the implementation of low-cost LIS panels. Nevertheless, the level of processing increases with the number of antennas, which is the case of the LIS (this can be viewed as a beyond-massive MIMO). Because of this, it is extremely important to study receivers that are as simple as possible. This article associates receivers with low complexity (that simplify the decoding process), with the use of a subset of the LIS panels, known as the partial LIS. By using a subset of the LIS panels, the decoding process becomes less complex, while the performance tends to be kept almost unchanged.

Block transmission techniques are commonly used to reduce intersymbol interference. The SC-FDE block transmission technique presents the advantage of exhibiting lower PAPR [14,15], as compared with OFDM, which makes it well suited for scenarios such as those involving an uplink and for facilitating the efficiency of the power amplification process [18].

Unlike traditional communications between a UE and a base station (BS), the communication between a UE and an LIS system is typically established in a line-of-sight scenario. The LIS can be viewed as a short-range beamformer, while the distance between antenna elements is typically half-wavelength, instead of three to four wavelengths, as in traditional MIMO systems. Moreover, while the individual antenna elements of the LIS establish communications in the far field, the whole array of the LIS system establishes communications in the near field, that is, shorter than the Fraunhofer distance, which is only a few wavelengths. This makes the LIS exhibit special properties. While in traditional beamforming, the focus is established along the azimuth and elevation planes, the LIS also allows for focusing along the distance plane. This property allows for a mitigation of the interference coming from users aligned in terms of azimuth and elevation but placed at different distances.

As depicted in Figure 1, the n th transmitted block, of N data symbols, sent by the t th UE is denoted as $s_n^{(t)}$, while the received block by the r th antenna of the LIS system is denoted as $y_n^{(r)}$. The mapping between the time domain signal and the frequency domain signal, for the k th subcarrier (assumed invariant during the transmission of a given block), of the transmitted block is defined as $DFT\{s_n^{(t)}; n = 0, 1, \dots, N - 1\} = \{S_k^{(t)}; k = 0, 1, \dots, N - 1\}$, i.e., by performing the discrete Fourier transform (DFT) of the time-domain block (a similar method applies, mutatis mutandis, to the received signal block, channel and noise).

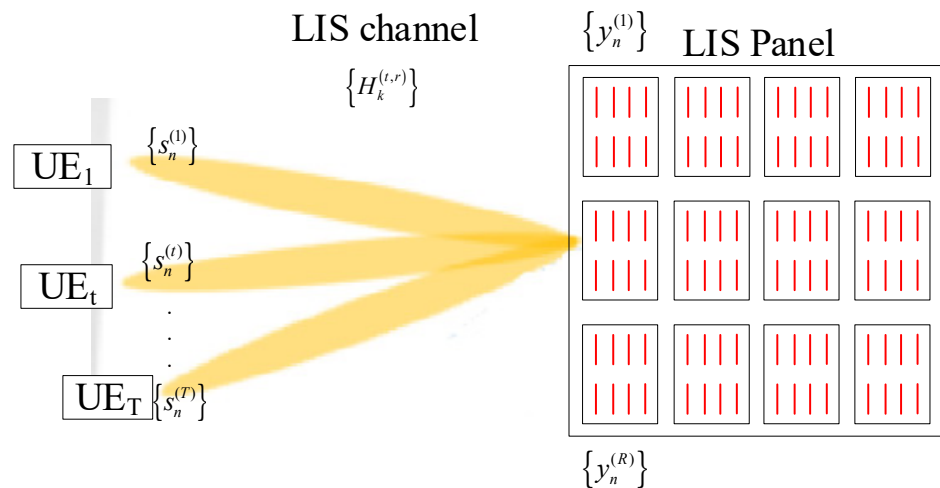


Figure 1. Block diagram of an LIS System.

The received frequency domain signal, in matrix–vector representation, becomes [14]

$$\mathbf{Y}_k = [Y_k^{(1)}, \dots, Y_k^{(R)}] = \mathbf{H}_k \mathbf{S}_k + \mathbf{N}_k \tag{1}$$

where $\mathbf{S}_k = [S_k^{(1)}, \dots, S_k^{(T)}]^T$ stands for the frequency-domain-transmitted data symbols, \mathbf{H}_k denotes the $T \times R$ channel frequency response for the k th subcarrier (assumed to be invariant during the transmission of a given block), with (r, t) th element $H_k^{(t,r)}$. Moreover, \mathbf{N}_k is the frequency-domain block channel noise for that subcarrier [14].

In this article it is assumed that only a subset of the LIS antennas is employed to create a beam towards the desired UE. This can be viewed from Figure 2, showing a partial LIS. The criterion utilized was the selection of the antennas that are closer to each UE.

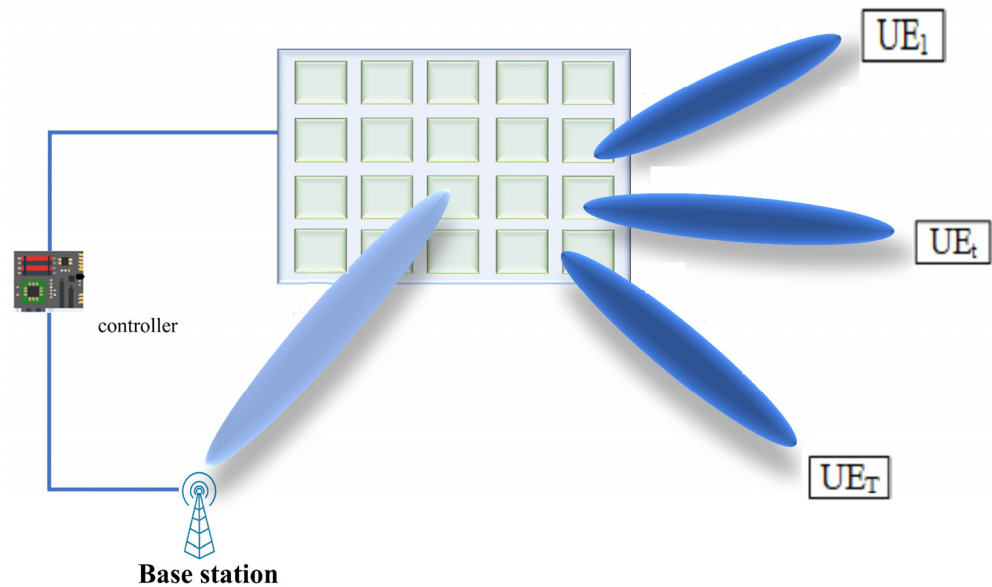


Figure 2. Block diagram of a partial LIS.

System and Signal Model for the Receivers

It is known that the ZF and MMSE receivers are complex, from a computation point of view, as they require a channel inversion for each frequency component. This translates into heavy battery use. The ZF receiver presents the advantage of intersymbol interference remotion that is undertaken in a very efficient manner. Nevertheless, it also has the disad-

vantage of presenting enhanced noise for average-to-high noise levels, which translates into a performance degradation. On the other hand, MRC and EGC receivers avoid such complexity, leading to a very simple receiver that is especially useful in an LIS scenario in which the number of antenna elements is extremely high. Nevertheless, MRC and EGC receivers generate some level of interference in the decoding process, which should be suppressed with iterative receivers.

Assuming a non-iterative receiver, the estimated frequency domain data symbols $\tilde{\mathbf{S}}_k = [\tilde{S}_k^{(1)}, \dots, \tilde{S}_k^{(R)}]^T$ become

$$\tilde{\mathbf{S}}_k = \mathbf{B}_k \mathbf{Y}_k \tag{2}$$

Depending on the algorithm, \mathbf{B}_k can be computed [16] as

1. Using the ZF receiver, \mathbf{B}_k becomes

$$\mathbf{B}_k = \mathbf{H}_k^H (\mathbf{H}_k \mathbf{H}_k^H)^{-1} \tag{3}$$

2. Using the MMSE receiver, \mathbf{B}_k becomes

$$\mathbf{B}_k (\mathbf{H}_k \mathbf{H}_k^H + \beta \mathbf{I})^{-1} \mathbf{H}_k^H \tag{4}$$

where $\beta = \frac{\sigma_N^2}{\sigma_S^2} = \frac{E[|N_k|^2]}{E[|S_k|^2]}$ and where \mathbf{I} is an $R \times R$ identity matrix.

3. Using the MRC receiver, \mathbf{B}_k becomes

$$\mathbf{B}_k = \mathbf{H}_k^H \tag{5}$$

4. Using the EGC receiver, \mathbf{B}_k becomes

$$\mathbf{B}_k = \exp \left\{ j \arg \left(\mathbf{H}_k^H \right) \right\} \tag{6}$$

A very efficient receiver commonly associated with SC-FDE schemes is the iterative block–decision feedback equalization (IB–DFE) [15]. Such an iterative receiver uses feedforward and feedback coefficients to process the signals in the frequency domain, reaching a performance that is typically much better than that of a non-iterative receiver. IB–DFE can be viewed as turbo equalization [15]. As described above, the MRC and EGC receivers are very simple from a computation point of view, but generate some residual interference in the decoding process, especially for moderate values of T/R . This can be mitigated by employing an iterative receiver, similar to the IB–DFE, that implements the following function [16]:

$$\tilde{\mathbf{S}}_k = \mathbf{B}_k^H \mathbf{Y}_k - \mathbf{C}_k \tilde{\mathbf{S}}_k \tag{7}$$

The interference cancellation matrix \mathbf{C}_k can be computed as [16]

$$\mathbf{C}_k = \mathbf{A}_k^H \mathbf{H}_k - \mathbf{I} \tag{8}$$

where \mathbf{I} is an $R \times R$ identity matrix.

3. Simulation Results and Analysis

This section shows the performance of the LIS and partial LIS, in terms of bit error rate (BER), as a function of E_b/N_0 . E_b stands for the energy of the transmitted bits, and N_0 is the one-sided power spectral density of the noise. Results are obtained through Monte Carlo simulations, using SC-FDE block transmission techniques. In the simulations, the locations of the users are randomly selected within the compartment. The channel has five multipath components (an LoS and four reflected rays in the walls) without fading, and

the power of each multipath component is given by the propagation conditions (overall propagation length plus reflection losses). Ground-reflected paths are more likely to be blocked and/or attenuated by the antennas' radiation pattern and have a lower reflection factor (for example, if a mat or a carpet is employed). It is worth noting that the number of reflections does not seem to have a significant effect on the performance and does not affect our main conclusions (the conclusions are essentially the same even with second-order reflections). In the Monte Carlo simulations, we considered $N = 256$ symbols, as a block size (we obtained similar results for other values of $N \gg 1$). Moreover, the QPSK modulation was adopted. In some scenarios, LDPC codes are utilised in the Monte Carlo simulations. When LDPC codes are used, these have a code rate of $\frac{1}{2}$. The length of the LPDC codes utilized in the simulations is 32,400 from the DVB-S.2 standard (also used in [10]). LDPC codes have gained significant attention due to their excellent performance in various communication systems, including wireless, satellite, and optical communication. These are characterized by their sparse parity-check matrices, which lead to efficient encoding and decoding algorithms. Regular LDPC codes were employed in the simulations, with all variable nodes and all check nodes having the same degree. In the simulations, we employed a min-sum belief propagation decoder with 20 iterations, using hard decision. Figure 3 shows a 3D user distribution map that allows for the viewing of the distribution of users and also the distribution of the panels, and which gives an idea of how much each user is aligned with each panel. Figure 3 also shows the scenario considered in the simulations, with four panels on the ceiling, each with a different number of antennas. Moreover, the number of users varies, depending on the scenario. Note that their locations are randomly selected by the simulation, i.e., each run of the Monte Carlo simulation considers a different location for the users.

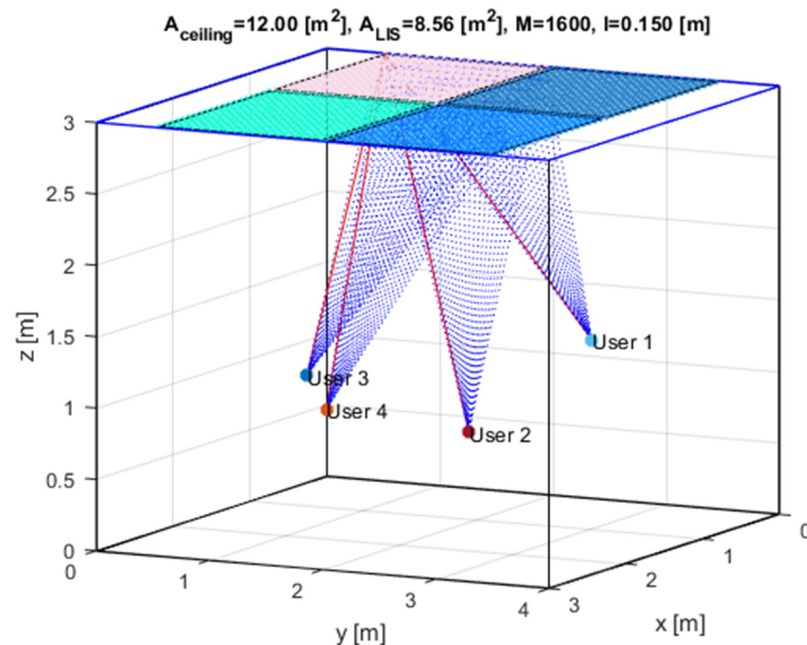


Figure 3. Scenario considered in the simulations with four panels.

Different graphics include results for “full LIS” and “partial LIS”. “Full-LIS” corresponds with the performance results of the regular LIS with all panels and all antennas in each panel. On the other hand, “partial LIS” means that such results with this designation correspond with the use of a subset of the total number of antennas that compose the LIS system. “Partial LIS” considers the antennas that are closer to each user while mitigating the level of interference of the other users. In other words, “full LIS” considers the total number of panels, and total number of antennas. In our simulations, we considered four panels. “Partial LIS—one panel” corresponds with the use of only one panel (the closest

panel) of the four total panels. In the other scenarios of “partial LIS” that do not correspond with the use of one panel, the number of antennas under consideration is stated. For example, in the configuration 4×400 , “full LIS” corresponds with 4 panels of 400 antennas on each panel, while “partial LIS—one panel” corresponds with the use of a single panel, i.e., 1×400 . Moreover, “partial LIS—225 antennas” corresponds with the use of only 225 of the $4 \times 400 = 1600$ antennas of the full LIS.

The different graphics representing the performances include matched filter bound (MFB) curves. These represent a lower bound in performance, corresponding with a scenario without intersymbol interference. In other words, this corresponds with the performance when a single symbol is transmitted and in which the degradation is due only to fading.

Figure 4 shows the performance results with the 4×400 LIS system, with 2 users, without LDPC codes, with and without the partial LIS. The 4×400 LIS system means that 4 panels of 400 antennas each are utilized (20 antennas on each side of the panel), making a total of 1600 antennas as part of the LIS. The number of users is 2, which means that there is one reference user and one interfering user. As can be seen, for the full LIS (i.e., with the use of 4 panels, each with 400 antennas), the ZF receiver has a performance slightly better than the MRC. Nevertheless, the MRC presents the advantage that the receiver is much simpler, as it does not require the channel inversion for each frequency component of the channel. When only a subset of the whole LIS is utilized (partial LIS), using only 225 antennas out of the total 1600, the performance achieved is much worse than that of the whole LIS, for both receiver types. Nevertheless, when the partial LIS comprises 361 antennas out of a total of 1600, one can see that the performance is slightly better than that of the full LIS. This occurs because the number of antennas utilized by the partial LIS (361) is sufficiently high, compared with the total (1600), enabling the exploitation of diversity. In addition, the slight gain of performance obtained with this configuration compared with the full LIS also results from the fact that a partial LIS allows interference mitigation. Similarly, observing the performance results achieved with “partial LIS—one panel”, the performance obtained is even better than that obtained with 361 antennas. Note that one panel corresponds with the use of the panel that is closer to each user, comprising 400 antennas (i.e., more than the previously considered 361 antennas), and, therefore, with the increasing gain obtained with the beam, while the ability to mitigate interference is kept. It is worth noting that the ZF receiver achieves a performance slightly better than that of the MRC receiver, in all scenarios, though at the cost of a higher complexity (processing at the receiver side).

Figure 5 shows the performance results with the 4×225 LIS system, with 2 users, without LDPC codes, and with and without the partial LIS. The 4×225 LIS system is one in which 4 panels of 225 antennas each are utilized (15 antennas on each side of the panel), making a total of 900 antennas as part of the LIS. Like the previous graphic, the number of users is 2, which means that there is one reference user and one interfering user. The “full LIS” corresponds with the use of the total of 900 antennas, while the “partial LIS—one panel” corresponds with the use of the panel (with 225 antennas) that is closer to each user, mitigating the interference. As can be seen, like the results of the previous figure, results obtained with “partial LIS—one panel” indicate improvement over the performance obtained with “full LIS”, for the different receiver types. This happens because the number of antennas per panel is still sufficiently high (225 antennas), allowing a good gain in terms of diversity, while mitigating the interference over the interfering user due to the use of a single panel, instead of the whole LIS. In terms of receiver types, one can see that ZF and MMSE receivers achieve the same performance, leading to the best results. This is followed by the low complexity MRC receiver, whose performance is always between those obtained with ZF/MMSE and EGC receiver. It is worth noting that, in the case of the “full LIS”, the performance obtained with the MRC receiver is almost superimposed over those obtained with the ZF/MMSE receivers, while in the case of the “partial LIS—one panel” the MRC shows a small degradation compared with the ZF/MMSE.

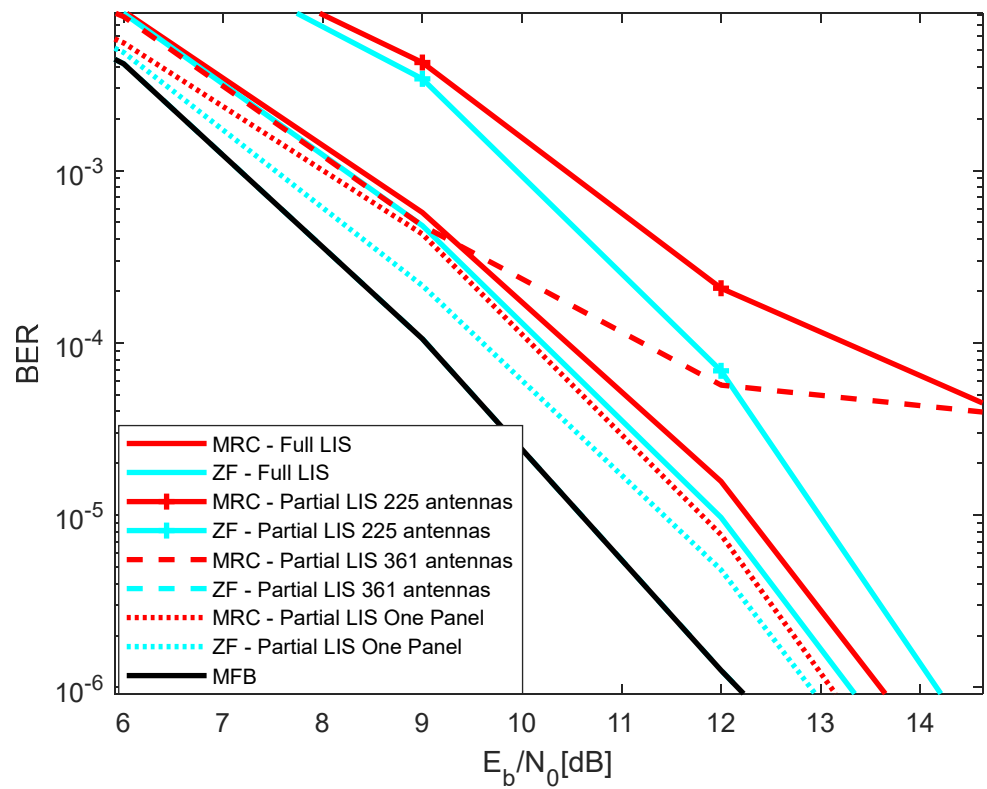


Figure 4. Performance results of the 4×400 LIS system, with 2 users, without LDPC codes, and with and without the partial LIS.

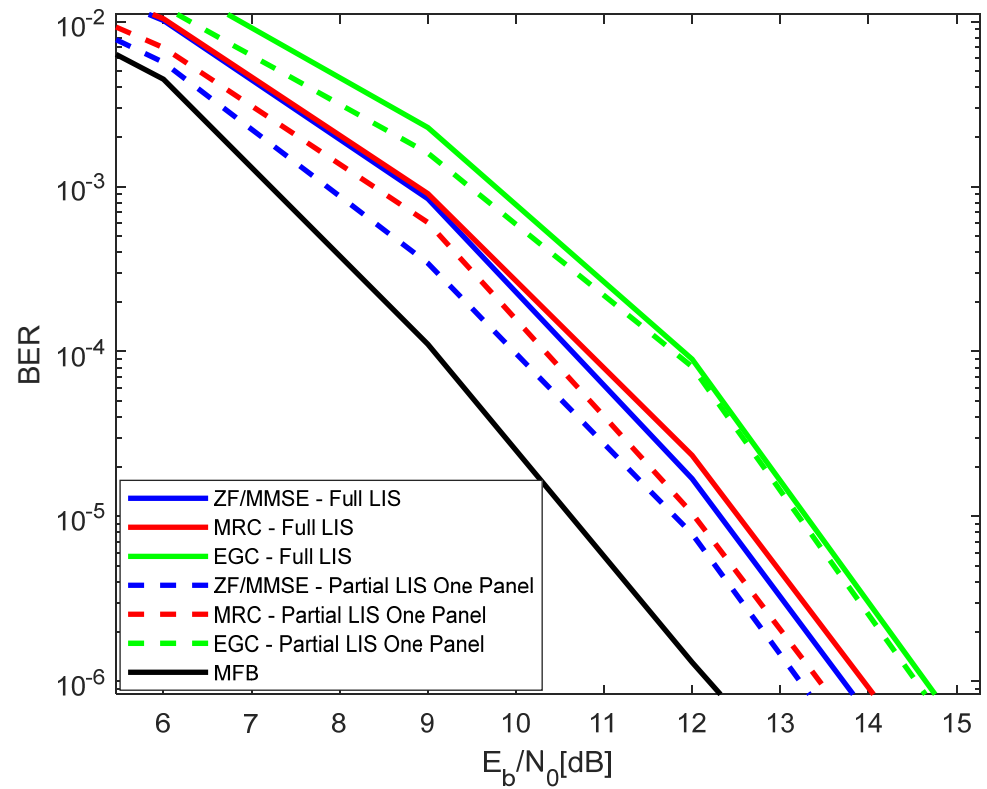


Figure 5. Performance results of the 4×225 LIS system, with 2 users, without LDPC codes, and with and without the partial LIS.

In the previous graphics, one can see that “partial LIS—one panel” achieves the best performance results, for both 4×400 LIS and 4×225 LIS. Figure 6 shows the results with a partial LIS, using a single panel, with 2 users, without LDPC codes, but while performing a comparison between different LIS configurations. As can be seen from Figure 6, the use of one panel with the configuration 4×400 LIS (i.e., with each panel corresponding to 1×400 LIS) slightly outperforms the configuration 4×225 LIS—one panel (i.e., 1×225), for all receiver types. Nevertheless, the results obtained with 4×50 LIS—one panel (i.e., 1×50) experience a significant degradation as compared with the other two LIS configurations, while the MRC and EGC receivers perform very badly. This occurs because the diversity gain obtained with the 50 antennas is very low.

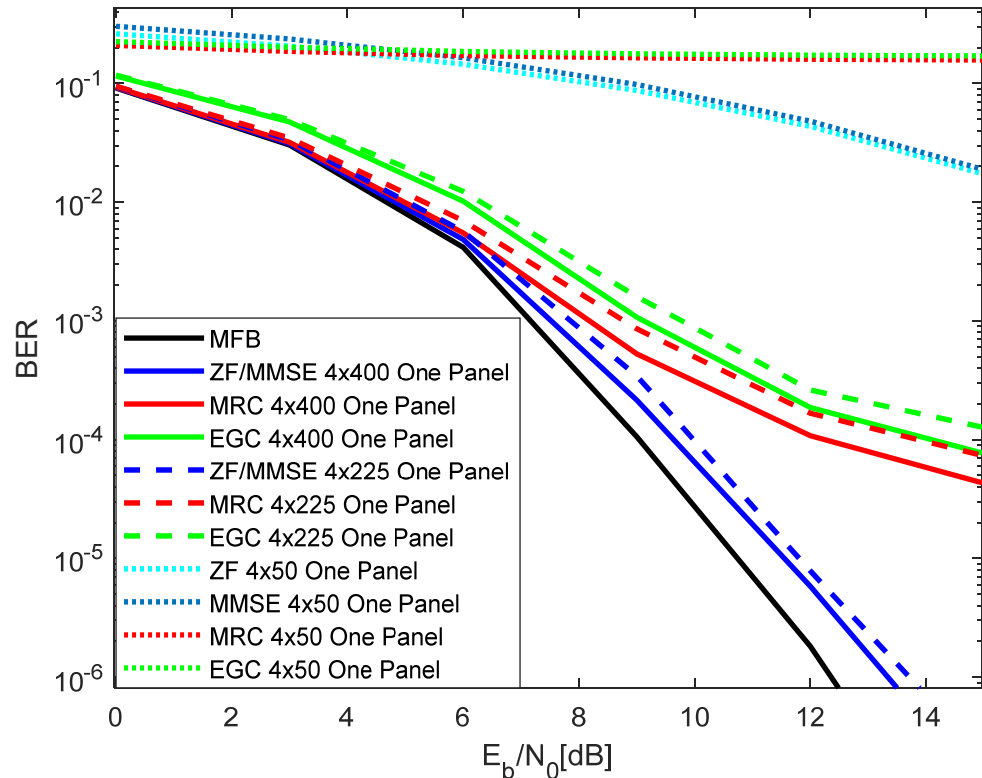


Figure 6. Performance results of several LIS configurations, with 2 users, without LDPC codes, with the partial LIS—one panel.

Figure 7 shows the performance results of the 4×400 LIS system, with 16 users, without LDPC codes, with and without the partial LIS. Similar to the results shown in Figure 4 (2 users), Figure 7 shows that, with 16 users and for this LIS configuration, the utilization of a single panel leads to a gain in performance as compared with the scenario of the full LIS configuration. Moreover, such gain is higher in the case of 16 users (Figure 7) than in the case of 2 users (Figure 4). This occurs because the use of one panel allows interference mitigation (as compared with the full LIS), whose effect is more visible for a higher number of interfering users.

Figure 8 shows the performance results of the 4×361 LIS system, with several number of users (2, 8 and 16 users), with the partial LIS, and without LDPC codes. As expected, the performance degrades with the increase in the number of users. Nevertheless, as previously shown, the performance degradation is partially mitigated using the partial LIS. Moreover, the performance degradation with the increase in the number of users is very low in the case of the ZF/MMSE receivers, which is achieved at the cost of a higher processing power, as compared with the MRC/EGC receivers.

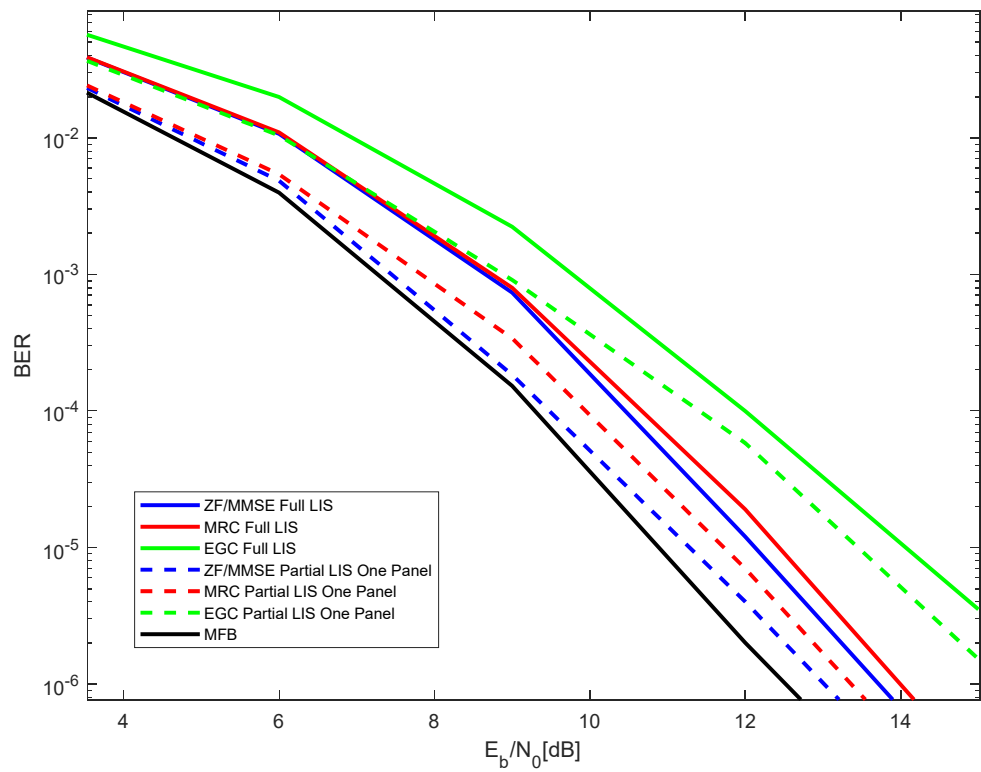


Figure 7. Performance results of the 4×400 LIS system, with 16 users, without LDPC codes, with and without the partial LIS.

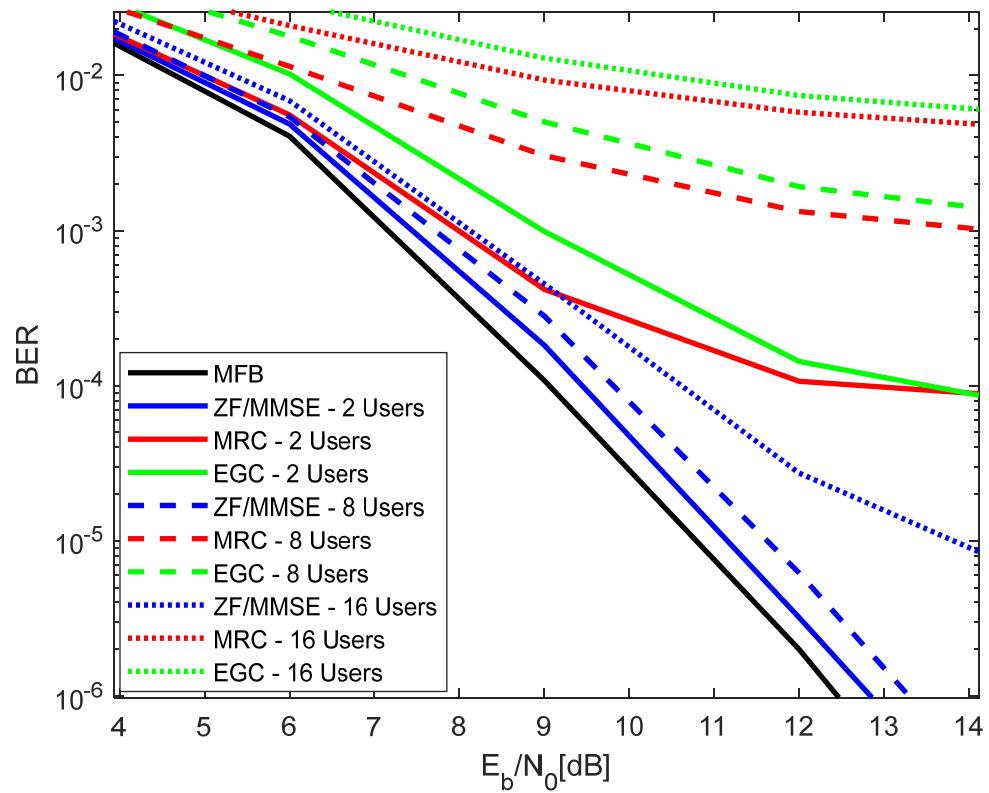


Figure 8. Performance results of the 4×361 LIS system, with several number of users, with the partial LIS, and without LDPC codes.

Figure 9 aims to perform a comparison between the results with and without LDPC codes. Note that the use of LDPC with the full LIS has been previously analysed in [10]. Figure 9 shows results like those of Figure 5 but in which the LDPC codes are also shown, considering the scenario with the partial LIS. One can see that the use of LDPC codes allows for a performance improvement for all receiver types, and with the partial LIS. Note that the partial LIS corresponds with the use of one panel. The gain achieved with the LDPC codes is of the order of 2 dB in the different scenarios.

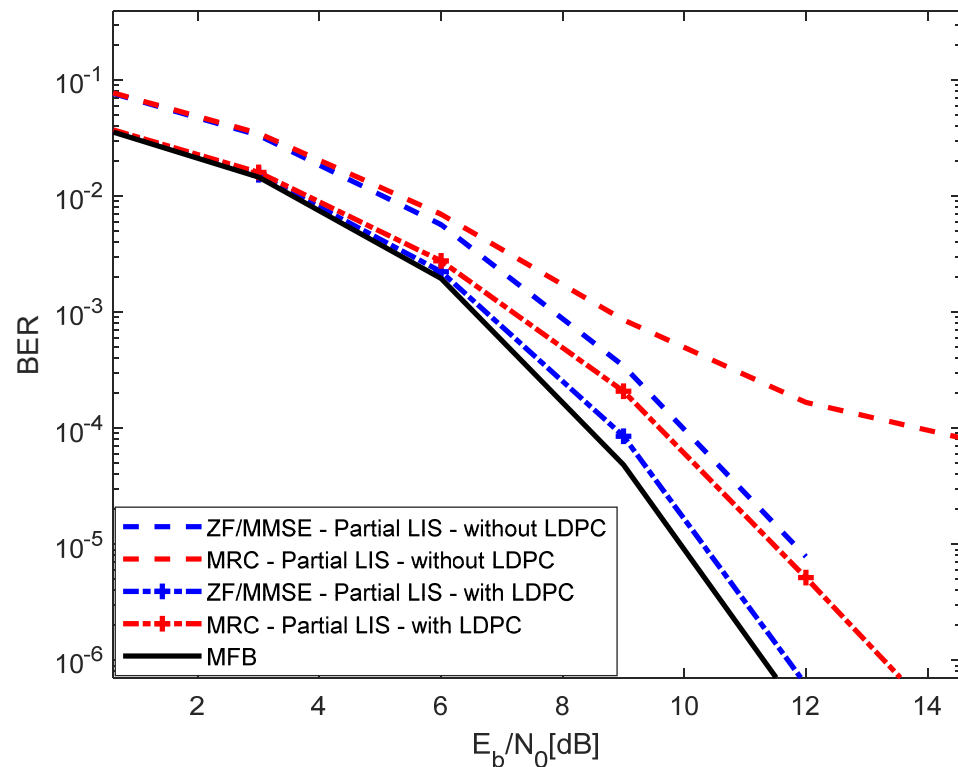


Figure 9. Performance results of the 4×225 LIS system, with 2 users, with and without LDPC codes, and with the partial LIS.

4. Conclusions

This article performs a comparison between the results with the full LIS, in different scenarios of antennas, and with the partial LIS, with and without LDPC codes. In the case of the partial LIS, different numbers of antennas are considered. It can be seen that, as long as the number of antennas that compose the LIS system is sufficiently high to provide a high level of diversity, the partial LIS with one panel tends to achieve the best overall performance. Different receiver types were analysed in the above-described scenarios, while the ZF/MMSE are those that tend to achieve the best performance and the MRC is the one that, performing slightly worse than ZF/MMSE, is very simple. This is because it avoids the computation of the channel inversion, for each frequency component of the channel, that is required for ZF/MMSE receivers.

Finally, one can see that the use of the partial LIS, associated with LDPC codes, tends to achieve the best overall performance, as long as the number of antennas that compose the LIS is sufficiently high to provide a high level of diversity. The partial LIS tends to outperform the full LIS because it allows for the mitigation of interference.

Considering the downlink scenario, future research should focus on the use of OFDM transmission techniques, instead of the SC-FDE adopted in this study.

Author Contributions: Investigation, M.M.d.S., A.G., R.D., G.P., A.C. and J.G. All authors have read and agreed to the published version of the manuscript.

Funding: This work is funded by FCT/MCTES through national funds and, when applicable, co-funded EU funds under the projects UIDB/EEA/50008/2020 and 2022.03897.PTDC.

Data Availability Statement: Data was obtained using Monte Carlo simulations and implemented using Matlab.

Acknowledgments: We acknowledge the support of FCT/MCTES, as described above in the funding section. We also acknowledge the support of Autonomia TechLab for providing an interesting environment in which to carry out this research.

Conflicts of Interest: The authors declare no conflicts of interest.

References

1. Kunze, L.; Hawes, N.; Duckett, T.; Hanheide, M.; Krajnik, T. Artificial Intelligence for Long-Term Robot Autonomy: A Survey. *IEEE Robot. Autom. Lett.* **2018**, *3*, 4023–4030. [\[CrossRef\]](#)
2. Mariani, M. Big IoT Data Analytics: Architecture, Opportunities, and Open Research Challenges. *IEEE Access* **2017**, *5*, 5247–5261.
3. Cabeças, A.; da Silva, M.M. Project Management in the Fourth Industrial Revolution. *TECHNO REVIEW Int. Technol. Sci. Soc. Rev.* **2021**, *9*, 79–96. [\[CrossRef\]](#)
4. Mu, X.; Xu, J.; Liu, Y.; Hanzo, L. RIS-Aided Near-field Communications for 6G: Opportunities and Challenges. *arXiv* **2023**, arXiv:2312.13004.
5. Decarli, N.; Dardari, D. Communication Modes with Large Intelligent Surfaces in the Near Field. *IEEE Digit. Object Identifier* **2021**, *9*, 165648–165666. [\[CrossRef\]](#)
6. Bjornson, E.; Özlem, T.; Sanguinetti, L. A primer on near-field beamforming for arrays and reconfigurable intelligent surfaces. In Proceedings of the 2021 55th Asilomar Conference on Signals, Systems, and Computers (ACSSC), Pacific Grove, CA, USA, 31 October–3 November 2021; pp. 105–112.
7. Ju, Y.; Cao, Z.; Chen, Y.; Liu, L.; Pei, Q.; Mumtaz, S.; Dong, M.; Guizani, M. NOMA-Assisted Secure Offloading for Vehicular Edge Computing Networks with Asynchronous Deep Reinforcement Learning. *IEEE Trans. Intell. Transp. Syst.* **2023**, 1–14. [\[CrossRef\]](#)
8. Zhu, L.; Zhang, J.; Xiao, Z.; Cao, X.; Xia, X.-G.; Schober, R. Millimeter-Wave Full-Duplex UAV Relay: Joint Positioning, Beamforming, and Power Control. *IEEE J. Sel. Areas Commun.* **2020**, *38*, 2057–2073. [\[CrossRef\]](#)
9. Dajer, M.; Ma, Z.; Piazzzi, L.; Narayan, P.; Qi, X.; Sheen, B.; Yang, J.; Yue, G. Reconfigurable Intelligent Surface: Design the Channel—A New Opportunity for Future Wireless Networks. *arXiv* **2020**, arXiv:2010.07408v1. [\[CrossRef\]](#)
10. Gashtasbi, A.; da Silva, M.M.; Dinis, R.; Guerreiro, J. On the Performance of LDPC-Coded Large Intelligent Antenna System. *Appl. Sci.* **2023**, *13*, 4738. [\[CrossRef\]](#)
11. Gashtasbi, A.; da Silva, M.M.; Dinis, R. IRS, LIS, and Radio Stripes-Aided Wireless Communications: A Tutorial. *Appl. Sci.* **2022**, *12*, 12696. [\[CrossRef\]](#)
12. Hu, S.; Rusek, F.; Edfors, O. Beyond Massive-MIMO: The Potential of Data-Transmission with Large Intelligent Surfaces. *arXiv* **2017**, arXiv:1707.02887v1. [\[CrossRef\]](#)
13. Pavia, J.P.; Velez, V.; Souto, N.; da Silva, M.M.; Correia, A. System-Level Assessment of Massive Multiple-Input–Multiple-Output and Reconfigurable Intelligent Surfaces in Centralized Radio Access Network and IoT Scenarios in Sub-6 GHz, mm-Wave, and THz Bands. *Appl. Sci.* **2024**, *14*, 1098. [\[CrossRef\]](#)
14. Borger, D.; Dinis, R.; Montezuma, P. Low complexity MRC and EGC based receivers for SC-FDE modulations with massive MIMO schemes. In Proceedings of the 2016 IEEE Global Conference on Signal and Information Processing (Global SIP), Washington, DC, USA, 7–9 December 2016; pp. 675–678.
15. da Silva, M.M.; Dinis, R.; Guerreiro, J. A Low Complexity Channel Estimation and Detection for Massive MIMO using SC-FDE. *Telecom* **2020**, *1*, 3–17. [\[CrossRef\]](#)
16. da Silva, M.M.; Dinis, R.; Aleixo, J.; Oliveira, L.M.L. On the Performance of LDPC-Coded MIMO Schemes for Underwater Communications Using 5G-like Processing. *Appl. Sci.* **2022**, *12*, 5549. [\[CrossRef\]](#)
17. da Silva, M.M.; Dinis, R.; Martins, G. On the Performance of LDPC-Coded Massive MIMO Schemes with Power-Ordered NOMA Techniques. *Appl. Sci.* **2021**, *11*, 8684. [\[CrossRef\]](#)
18. Wang, J.; Baykas, T.; Funada, R.; Sum, C.S.; Rahman, A.; Lan, Z.; Harada, H.; Kato, S. A SNR Mapping Scheme for ZF/MMSE Based SC-FDE Structured WPANs. In Proceedings of the VTC Spring 2009—IEEE 69th Vehicular Technology Conference, Barcelona, Spain, 26–29 April 2009.

Disclaimer/Publisher’s Note: The statements, opinions and data contained in all publications are solely those of the individual author(s) and contributor(s) and not of MDPI and/or the editor(s). MDPI and/or the editor(s) disclaim responsibility for any injury to people or property resulting from any ideas, methods, instructions or products referred to in the content.